

Case Report

Rapid SO₂ gas removal using MgO/AC /CaCO₃/Zeolite nanocomposite at room temperatureGhobad Behzadi pour ^{a,*}, Maryam Kamel Oroumiyeh ^b, Leila Fekri aval ^b^a Department of Physics, East Tehran Branch, Islamic Azad University, Tehran, Iran^b Quantum Technologies Research Center, Science and Research Branch, Islamic Azad University, Tehran, Iran

ARTICLE INFO

Keywords:

SO₂
Adsorbent film
Efficiency
Adsorption capacity
Gas removal

ABSTRACT

The rising population and the expansion of urban areas are leading to heightened energy demands, which are predominantly met through fossil fuel sources. The operation of combustion facilities generates detrimental flue gases, thereby necessitating investigations into methods for controlling emissions to safeguard public health and protect the environment. The adsorbent method of removing pollutant gases involves selecting the proper material, preparation of the adsorbent layer, understanding adsorption mechanisms, contact time, and monitoring levels of pollutants. Various types of adsorbent materials are utilized, including active carbon (AC), zeolites, and metal oxides; each has different properties that affect the efficiency of pollutant removal. This research examined the MgO/AC/CaCO₃/Zeolite nanocomposite for SO₂ gas removal. The characterization of the adsorbent layer was conducted using X-ray diffraction (XRD), scanning electron microscopy (SEM), and Brunauer-Emmett-Teller (BET) analysis techniques. The findings demonstrated a swift decline in SO₂ level, which decreased from 153 ppm to 15 ppm in a short time of 5 minutes. The MgO/AC/CaCO₃/Zeolite film can considerably remove the SO₂ gas with an efficiency of 92 % at room temperature. The adsorbent film exhibited an adsorption capacity of 133 mg g⁻¹ within 5 minutes. The results of this study provide important insights into the removal of SO₂ gas by using adsorption layers, demonstrating the potential of MgO/AC/CaCO₃/zeolite nanocomposites as effective materials for air pollution control. This nanocomposite can effectively reduce SO₂ with fast adsorption time. As air quality standards continue to be tightened around the world, innovative materials can play a significant role in reducing harmful emissions from industrial sources.

1. Introduction

The increasing population and urban expansion are driving a surge in energy requirements, predominantly satisfied by fossil fuel sources, despite progress in renewable energy technologies. Combustion power plants emit flue gases that significantly contribute to air pollution and pose risks to public health and ecological systems. Various traditional and innovative technologies are under investigation to effectively manage and mitigate these harmful emissions. Consequently, numerous studies are conducted annually on pollutant gas removal using various techniques. SO₂ gas is an air pollutant produced by industrial activities, power generation, and transportation. It plays a role in acid rain formation and poses serious health risks. Research focused on the fast removal of SO₂ gas is crucial because of its potential effects on the environment, energy efficiency, adaptability for various industrial uses, and its role in promoting sustainable development. The research on SO₂

gas marks a notable step forward in finding effective ways to combat air pollution and encourages the advancement of innovative technologies in materials science. Fig. 1 illustrates the cumulative growth of published articles indexed in Scopus for gas pollution removal. The significant rise in published articles on gas pollution removal can be linked to several factors, including growing environmental awareness, technological advancements, collaboration across disciplines, and global climate initiatives. Examining co-occurring keywords related to gas pollution in scholarly articles, performed with VOSviewer is illustrated in Fig. 2. The comparative schematic of keywords taken from publications indexed in Scopus regarding gas pollution removal serves as a useful analytical tool. It deepens our understanding of current research priorities and highlights trends, gaps, new absorbent materials, and technologies. In summary, this schematic offers insights that can help drive progress in the field and enhance strategies for effectively managing gas pollution.

Current pollution control technologies, like selective catalytic

* Corresponding author.

E-mail addresses: ghobadbehzadi@yahoo.com (G. Behzadi pour), elmira.kamel@gmail.com (M. Kamel Oroumiyeh), leila2mst@yahoo.com (L. Fekri aval).

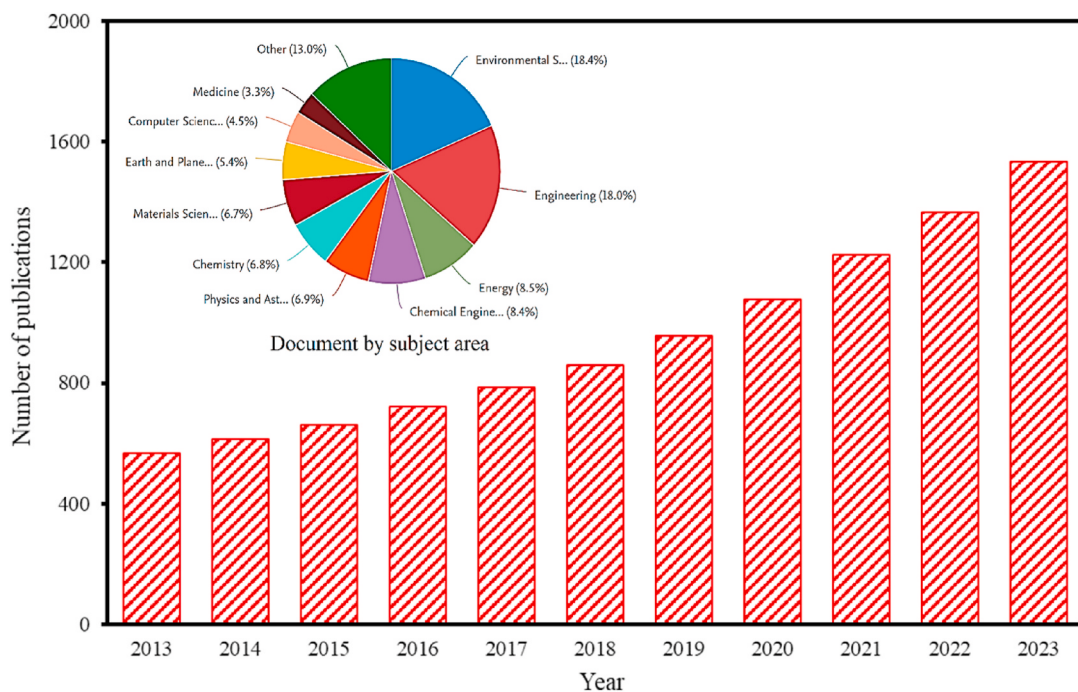


Fig. 1. The cumulative growth of published articles indexed in Scopus for gas pollution removal.

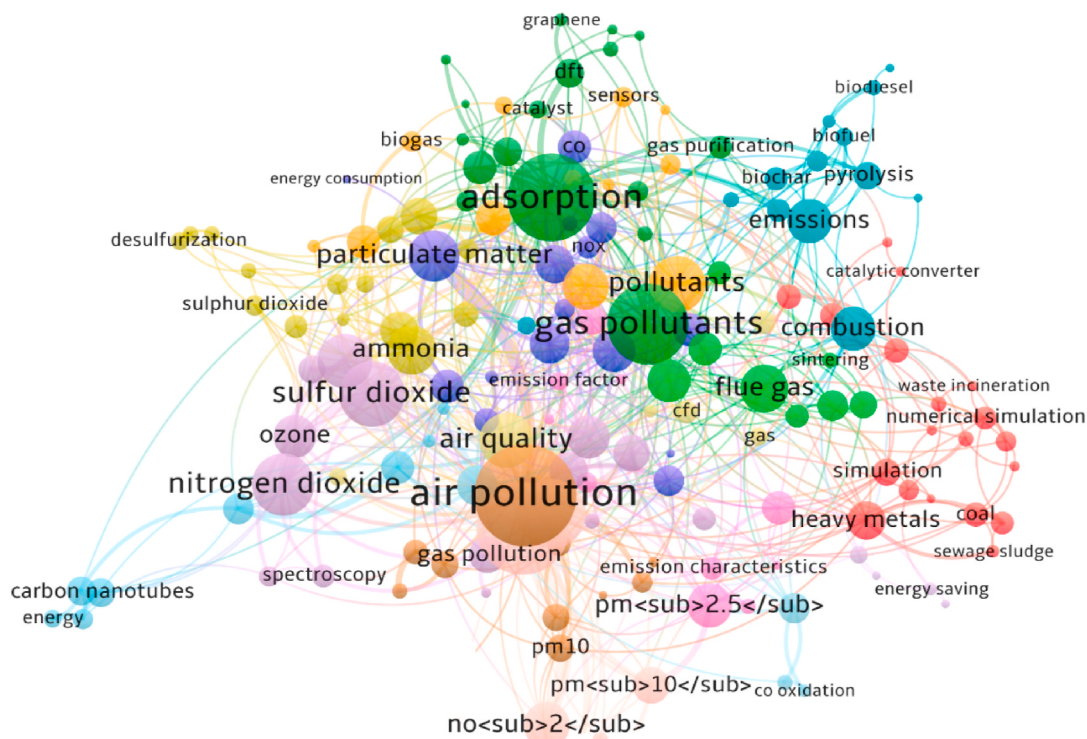


Fig. 2. The keywords of gas pollution removal from Scopus publications: (Scopus database).

reduction for nitrogen oxides, wet flue gas desulfurization for sulfur oxides, and electrostatic precipitators for particulate matter, have proven effective but also encounter challenges such as complexity, high costs, and the production of harmful by-products. Recent studies highlight advancements in carbon capture technologies, energy generation, and targeted emission management techniques aimed at specific pollutants, including sulfur-based compounds, nitrogen oxides, and carbon dioxide [1]. The challenges related to SO₂ gas pollutants are complex

and cover various aspects, including health, environmental impact, regulations, and technology. Tackling these challenges demands a collaborative approach from governments, industries, and communities, as well as ongoing improvements in monitoring and mitigation technologies to safeguard public health and the environment. Fig. 3 illustrates various technologies used to reduce gas pollution. Coal-fired power plants utilize methods like wet flue-gas desulfurization and selective catalytic reduction to lower SO₂ emissions. However, these

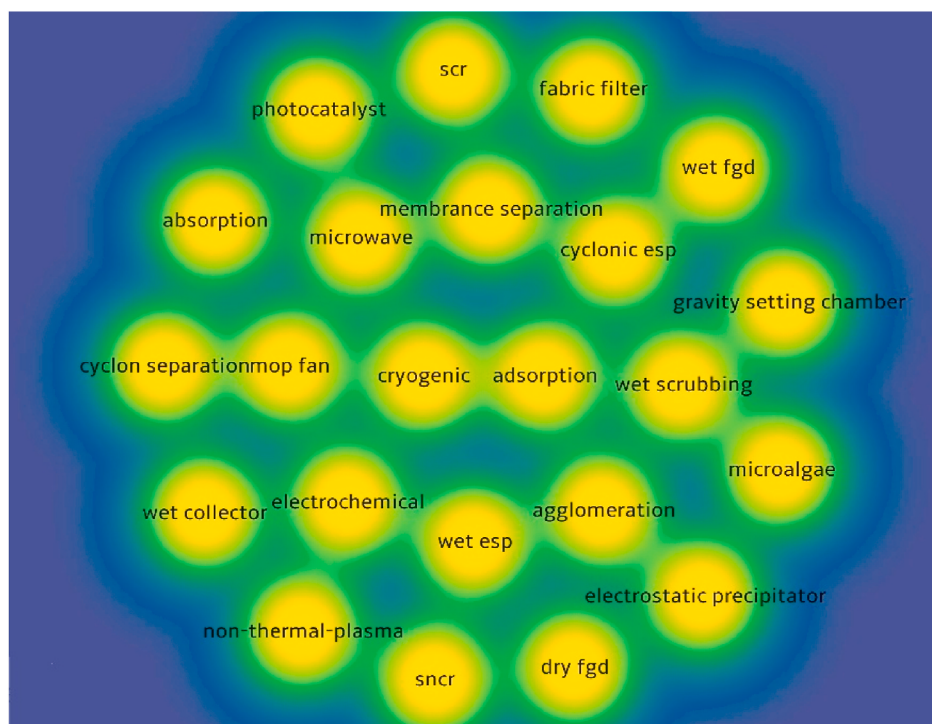


Fig. 3. Removal technology for gas pollution.

techniques can come with high operational costs and may lead to secondary pollution issues.

Novel ecological technologies and materials are being researched and developed, including advanced methods for air pollution mitigation, such as adsorption techniques [2]. Numerous studies have examined the efficacy of various adsorbents, including activated carbon (AC) [3], biochar, fibers, and mineral materials [4] in removing pollutants such as SO_2 and NO_x . Traditional adsorbents like AC have limitations in removing certain pollutants, leading to the investigation of new carbon-based materials, such as graphene oxide (GO), for air purification. The use of GO nanocomposites, especially GO/polyvinyl alcohol (PVA) membranes, has shown great promise in effectively capturing pollutants like formaldehyde and sulfur dioxide from indoor spaces [5]. A study used a thin nanocomposite adsorbent film based on AC, magnesium oxide, iron oxide, titanium dioxide, zinc oxide, and zeolite for SO_2 gas pollution removal [6]. That study showed an efficiency of 92 %

at room temperature. Nanocomposites are also used for monitoring gas concentrations in sensors [7–11] and energy storage devices [12,13].

Activated coke is a cost-effective and efficient adsorbent used for purifying flue gas pollutants. It has strong crushing strength and renewable properties, making it ideal for power plants and various industries to remove flue gas contaminants [14,15]. A study focused on urea peroxide as a potential adsorbent for the removal of SO_x , highlighting its benefits such as manageable oxidation processes, stability, and cost-effectiveness [16]. The effectiveness of urea peroxide in eliminating this pollutant from exhaust gases is subject to various influencing factors, including temperature, the presence of metal ions, and the concentrations of reactants. Yu et al. [17] noted that combining ionic liquids with porous materials offers a promising method for eliminating indoor pollutants. They pointed out that although materials based on ionic liquids showed considerable adsorption capacity for individual gases in complex settings, their limitation in simultaneously adsorbing

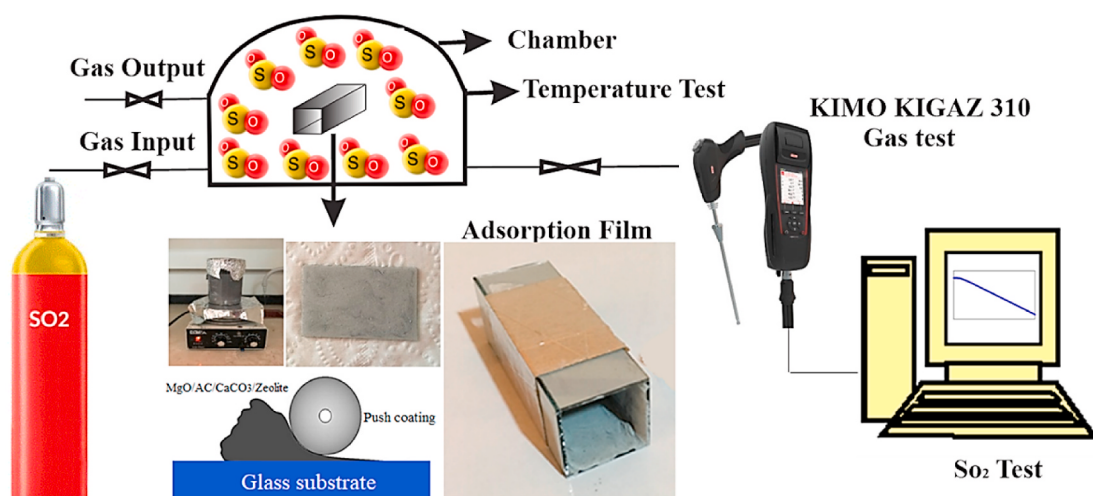


Fig. 4. The schematic configuration for the SO_2 gas test.

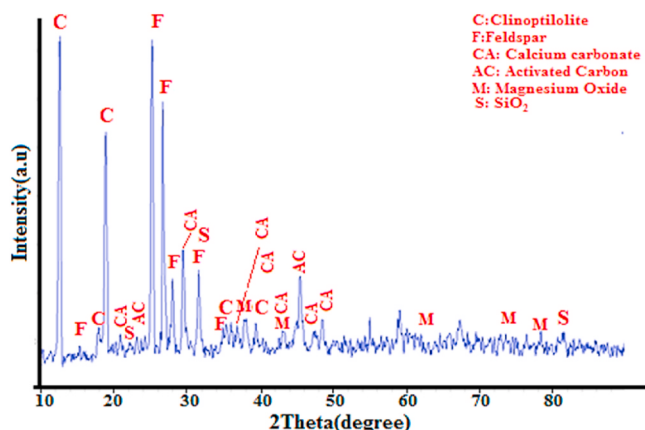


Fig. 5. The XRD diffraction pattern of the MgO/AC/CaCO₃/Zeolite nanocomposite.

multiple gases underscores an important area for future research.

Another study reported that a wet flue gas desulfurization method can remove SO₂ pollutants with an efficiency of 99.25 % [18]. Xia et al. [19] introduced an innovative wet-scrubbing technique utilizing Fe (VI) for the concurrent elimination of gaseous NO and SO₂. They assessed the practicality of continuously feeding ferrate for the simultaneous removal of multiple gaseous pollutants in a laboratory setting, achieving over 90 % removal efficiency for NO and complete removal of SO₂ at room temperature and under ambient conditions. The effectiveness of CaO and CaSO₄ in removing SO₂ at 900 °C and 90 % efficiency has been investigated in Ref. [20]. The gas pollution effectively capture heat emitted from the Earth's surface, resulting in elevated temperatures and a range of associated impacts. The results of a research investigation indicated that the process of ammonia scrubbing applied to flue gases achieves a sulfur dioxide removal efficiency of 99 % [21].

Adsorbents can be effective in removing SO₂ gas pollutants, but several parameters need to be considered. These challenges include adsorption capacity, operating temperature, fast time, efficiency, and the need for precise material selection. Addressing these parameters

through ongoing research and development is essential to improve the performance and applicability of SO₂ adsorbents in air quality management. This study investigates the efficacy of absorbent film combined with MgO/AC/CaCO₃/Zeolite composite to eliminate SO₂ gas pollutants at room temperature. The experimental results indicated that the film successfully reduced SO₂ levels by 92 % and an adsorption capacity of 138 mg g⁻¹ in 5 minutes, offering hope for future pollution control efforts.

2. Materials and methods

The MgO/AC/CaCO₃/Zeolite nanocomposite synthesis was created by dissolving Zeolite (1.5 g) and MgO (1 g), AC (1 g), and CaCO₃ (1 g) in distilled water (200 ml). The Zeolite utilized, belonging to the aluminosilicate class, is defined by the chemical formula (Al₂O₃)_x(SiO₂)_y·wH₂O. For the gas analysis, the nanocomposite was coated onto a glass substrate. The experimental configuration utilized for the SO₂ gas test is illustrated in Fig. 4. The KIMO KIGAZ Model 310 was employed for the analysis of SO₂ gas. This model is designed for flexibility, with interchangeable sensors, which are suitable for several applications in combustion analysis for accurate measurements to successfully monitor and comply with current environmental standards. It makes exacting measurements of SO₂ with its advanced measuring features. Measurement is offered in a range from 0.00 ppm up to 5000.00 ppm for thorough SO₂ concentration monitoring. Accuracy is stated at ±5 ppm or ±5 % of the reading, whichever is greater, making it fit for the acquisition of reliable and accurate data for compliance with environmental regulations.

For structural examination, the X-ray diffraction (the XRD model STOE) was carried out at Bragg angles (2θ) ranging from 5 to 90°, utilizing copper (Cu) as the radiation source, which has a wavelength of λ = 1.54 Å. Fig. 5 shows the XRD pattern related to the nanocomposite. The analysis of the XRD pattern reveals that the zeolite sample comprises three predominant phases: clinoptilolite, feldspar, and a silicon dioxide (SiO₂) crystal phase, which is denoted by the symbols C, F, and S, respectively. MgO exhibiting a cubic crystal structure presents diffraction peaks at angles of 37, 42, 62, 75, and 78°, which are associated with the (111), (200), (220), (311), and (222) crystal planes, respectively. The sharp peaks indicate that the nanocomposite with high

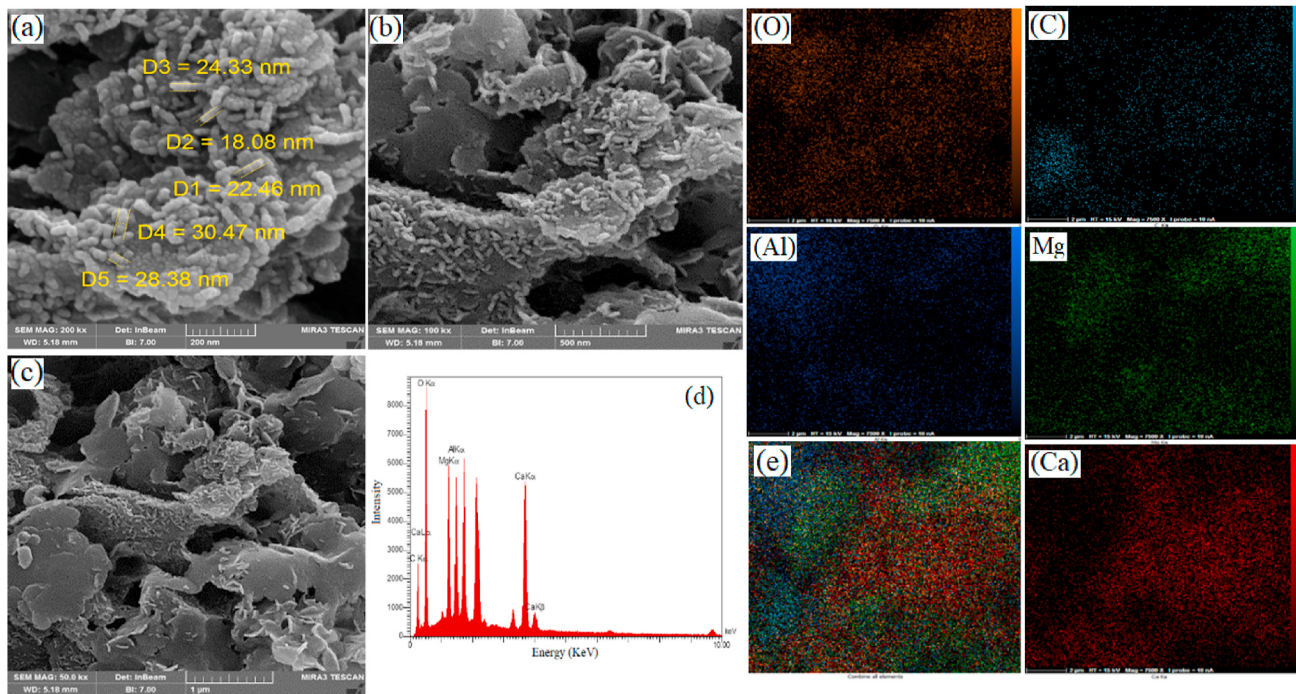


Fig. 6. (a–c) SEM images in different scales (d) EDX analysis (e) mapping analysis of the MgO/AC/CaCO₃/Zeolite nanocomposite adsorbent.

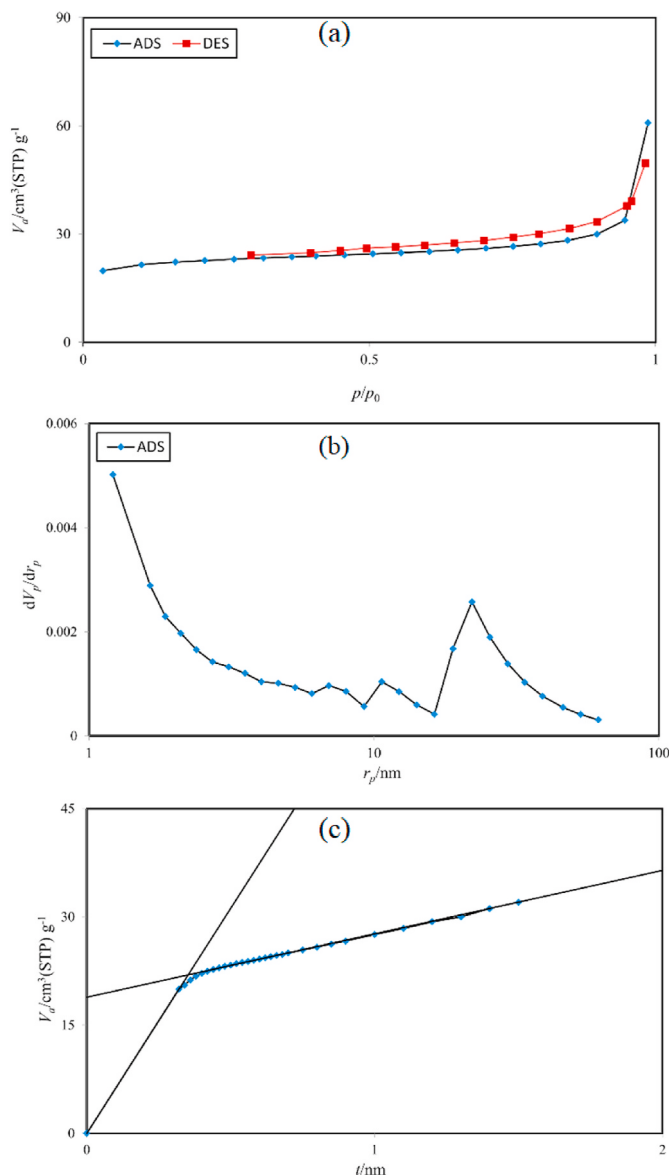


Fig. 7. Shows the BET analysis of the MgO/AC/CaCO₃/Zeolite nanocomposite (a) adsorption/desorption isotherm (b) BJH-plot (c) t-plot.

crystallinity was obtained under synthetic conditions, the width of the bands also indicates that the synthesized particles are nano-sized. The CaCO₃ sample exhibiting the calcite crystalline phase demonstrates diffraction patterns at angles of 23, 29, 36, 39, 43, 47, and 49°, which align with the (012), (104), (110), (013), and (013) crystal planes, respectively. Additionally, the reflections at (202), (018), and (016) are also noted. The observed narrowness of the diffraction bands further substantiates the presence of crystallites within the nano-sized phase.

3. Results and discussion

Fig. 6 presents the SEM images obtained using a TESCAN VEGA 3 device from the United States, alongside Energy Dispersive X-ray (EDX) and mapping analysis of the AC/CaCO₃/Zeolite nanocomposite adsorbent. EDX microanalysis is a specialized technique in electron microscopy that facilitates elemental analysis by generating characteristic X-rays, which yield insights into the elemental composition of the samples. Furthermore, the EDS analysis of the AC/CaCO₃/Zeolite nanocomposite reveals the weight percentages of various elements, specifically carbon (C) at 12.80 %, oxygen (O) at 39.51 %, aluminum (Al) at 15.81 %, (Mg)

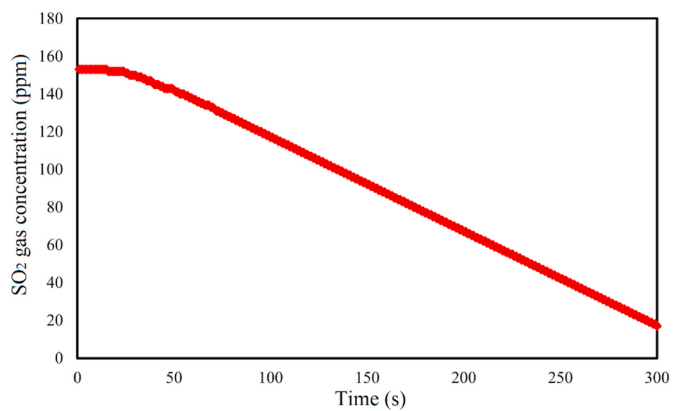


Fig. 8. Adsorption curve of SO₂ gas as a function of time.

at 15.41 %, and calcium (Ca) at 16.48 %. **Fig. 7** illustrates the SEM images, EDX, and mapping analysis of the MgO/AC/CaCO₃/Zeolite nanocomposite adsorbent.

The EDS examination of the MgO/AC/CaCO₃/Zeolite nanocomposite indicates the weight percentages of several elements C, O, Al, Mg, and Ca were 12.80 %, 39.51 %, 15.81 %, 15.41 %, and 16.48 %, respectively. The BET method is a prominent analytical technique employed in the fields of materials science and engineering for the determination of the specific surface area of porous substances, including catalysts, adsorbents, and powders. This methodology entails the adsorption of gas molecules onto the surface of the material, followed by the measurement of gas adsorption at varying pressures. The collected data is then analyzed and fitted to an isotherm model, which facilitates the calculation of the overall surface area of the material. **Fig. 7** shows the BET analysis of the nanocomposite. The BELSORB device did this analysis. The blue data points represent the absorption curve, while the red data points correspond to the desorption curve. The proximity of these curves, particularly at the intersection point which lies below 0.5, indicates the presence of very small diameters. By IUPAC classification, this particular curve is categorized as type 2. The structural cavities are characterized as sheets and cylinders that are closed on one end. The BET surface area is measured at 84.12 m² g⁻¹, whereas the Longmore surface area is recorded at 114.9 m² g⁻¹. The Barrett-Joyner-Halenda (BJH) analysis technique is employed to investigate the pore size distribution within porous substances, encompassing both micropores and mesopores. This analytical approach is fundamentally based on the adsorption and desorption isotherms derived from BET analysis. The BJH curve indicates that the pore radius measures 1.21 nm, while the volume of the internal cavity, denoted as V_p, is calculated to be 0.063026 cm³ g⁻¹. The t-plot technique is extensively utilized for a variety of materials, demonstrating its highest reliability for those exhibiting Type II or Type IV isotherms, particularly when there is a significant interaction between the adsorbate gas and the material's surface.

This method seeks to correlate the adsorption characteristics of a material with an idealized curve that represents the thickness of the adsorbed layer on the surface. To create the t-plot, isotherm loading data is plotted against thickness values derived from the model. Ideally, if the experimental adsorption curve aligns with the model, the resulting plot will yield a straight line that intersects the origin. However, due to the inherent discrepancies between adsorption occurring within the pores and that on the ideal surface, the t-plot often exhibits deviations that can be interpreted to reveal specific material properties. Notably, a pronounced vertical deviation suggests condensation within a particular pore type, while a more gradual slope indicates adsorption occurring along the walls of a specific pore. The analysis of the t-plot curve reveals that the external surface area of the pores measures 13.536 m² g⁻¹, while the internal surface area of the pores is quantified at 82.601 m²

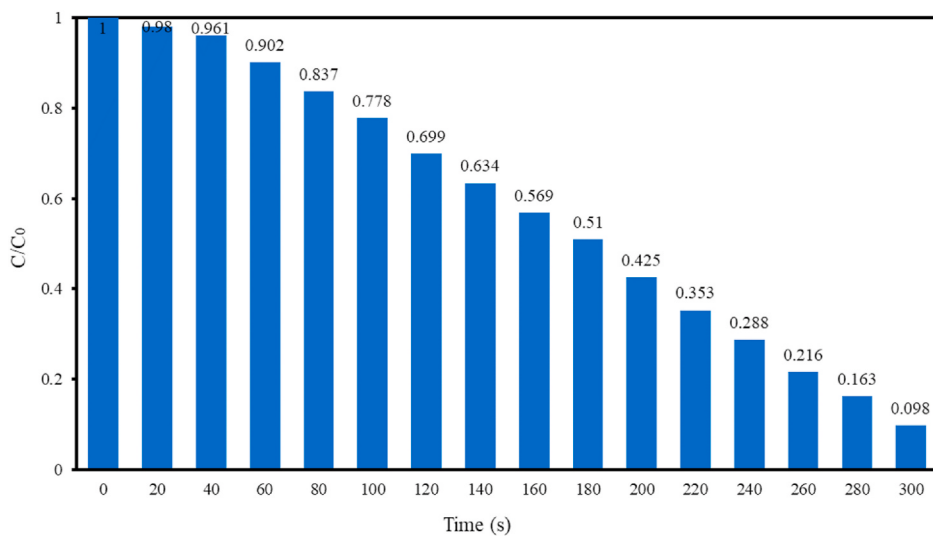


Fig. 9. The ratio of concentration to initial concentration versus time.

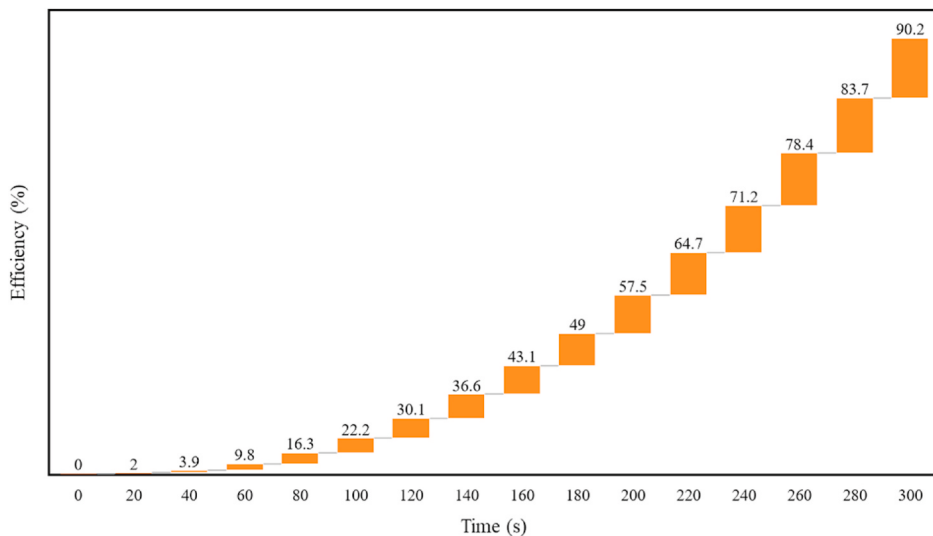


Fig. 10. The efficiency of $\text{MgO}/\text{AC}/\text{CaCO}_3/\text{Zeolite}$ adsorbent film for SO_2 .

g^{-1} . The temporal variation of SO_2 concentration was illustrated for the $\text{MgO}/\text{AC}/\text{CaCO}_3/\text{Zeolite}$ film, as depicted in Fig. 8. A thorough examination of the curve indicates a significant reduction in SO_2 concentration, decreasing from 153 ppm to 15 ppm for 300 seconds.

In the appraisal of pollutant removal through the application of sorbent materials, the ratio of (C/C_0) serves as a critical metric. Fig. 9 illustrates the plotted ratio of C/C_0 . After 300 seconds, the ratio of C/C_0 was measured to be 0.098. The efficiency of $\text{MgO}/\text{AC}/\text{CaCO}_3/\text{Zeolite}$ adsorbent can be determined by Ref. [22]:

$$E (\%) = \frac{(C_0 - C)}{C_0} \times 100 \quad (1)$$

Fig. 10 illustrates the efficiency of the $\text{MgO}/\text{AC}/\text{CaCO}_3/\text{Zeolite}$ composite adsorbent film in the removal of SO_2 gas. The efficiency indicates that after 300 seconds, the adsorbent film has successfully eliminated 90.2 % of the SO_2 gas at room temperature.

The adsorption capacity of an adsorbent layer can be determined by Ref. [22]:

$$Q_e = \frac{(C_0 - C_e) \times V}{M} \quad (2)$$

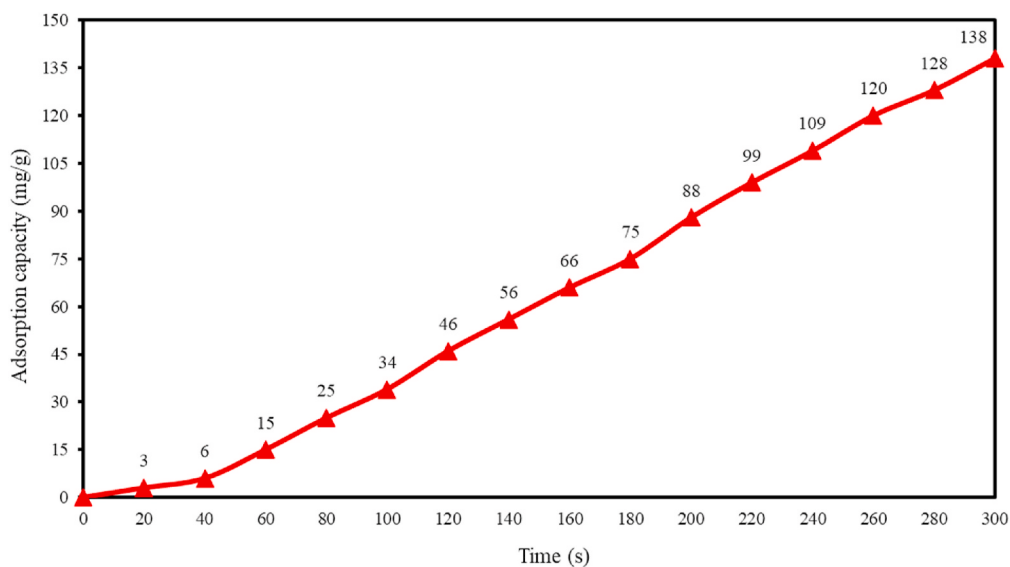
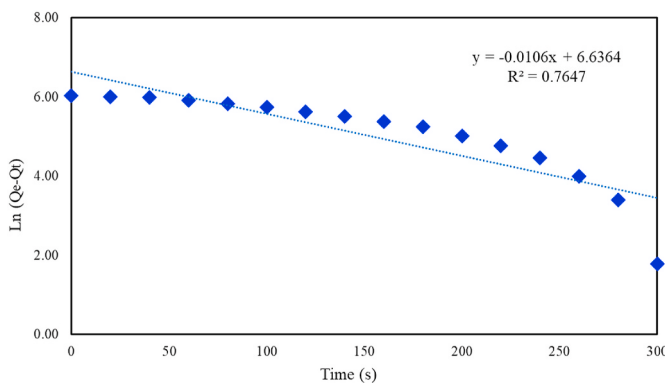
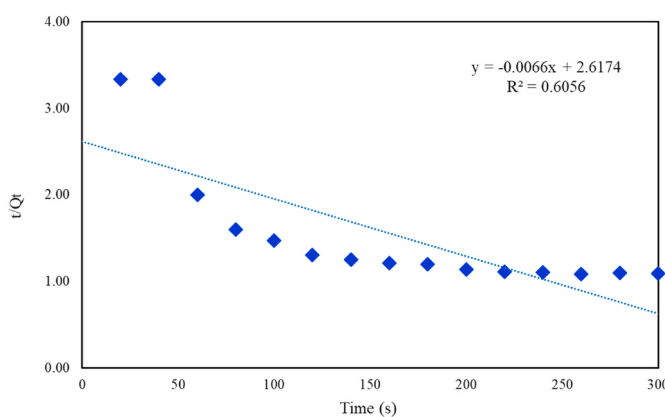
The chamber's volume is represented by the parameter V , whereas the mass of the adsorbent is indicated by M . Fig. 11 demonstrates the adsorption capacity of the adsorbent film. The information depicted in Fig. 11 distinctly demonstrates that the capacity for SO_2 gas adsorption reaches 138 mg g^{-1} following a duration of 300 seconds.

The kinetics of gas adsorption onto nanocomposite films were investigated using a pseudo-first-order model [23,24]. This model describes the kinetics of adsorption phenomena in terms of the fact that the rate of variation of the solute concentration is directly proportional to the difference between the saturation concentration and the amount adsorbed at any time [25,26].

$$\ln(Q_e - Q_t) = \ln(Q_e) - K_1 t \quad (3)$$

$$Q_t = \frac{(C_0 - C_t) \times V}{M} \quad (4)$$

Where Q_t is the amount adsorbed at time t , Q_e is the amount adsorbed at equilibrium, and K_1 is the pseudo-first-order rate constant. The slope of the linear plot of $\ln(Q_e - Q_t)$ versus t gives the value of $-K_1$. It allows the researcher to calculate the kinetic parameters from experimental data effectively. Fig. 12 shows a linear plot of $\ln(Q_e - Q_t)$ as a function of time.

Fig. 11. SO_2 adsorption capacity at room temperature.Fig. 12. Linear plot of $\ln(Q_e - Q_t)$ as a function of time.Fig. 13. Linear plot of t/Q_t as a function of time.

From Fig. 12, the pseudo-first-order rate constant K_1 was equal to 0.0106 s^{-1} .

The pseudo-second-order kinetic model might be applied to describe the adsorption kinetics of substances like SO_2 gas on adsorbent materials of $\text{MgO}/\text{AC}/\text{CaCO}_3/\text{Zeolite}$ nanocomposites. This assumes that the rate of adsorption is directly proportional to the square of the amount of adsorbate adsorbed at any given time. More precisely, it is supposed that

the adsorption might involve a chemical reaction that includes valence forces by sharing or exchanging electrons. The pseudo-second-order model is defined as follows [26]:

$$\frac{t}{Q_t} = \frac{1}{K_2 Q_e^2} + \frac{t}{Q_e} \quad (5)$$

Where $K_2 (\text{g mg}^{-1} \text{ s}^{-1})$ is the pseudo-second-order rate constant. The linear t/Q_t as a function of time gives intercept $1/K_2 Q_e^2$ and slope $1/Q_e$, to determine K_2 . Fig. 13 shows the plot of t/Q_t as a function of time and exhibits that the value of the pseudo-second-order rate constant is equal to $1.67 \times 10^{-5} \text{ g mg}^{-1} \text{ s}^{-1}$.

A significant value of K_1 compared to K_2 is indicative of a more dominant physisorption. With a better-fit R^2 value in the case of the pseudo-first-order model, this model explains greater variance of the experimental data than the pseudo-second-order model. Therefore, the pseudo-first-order kinetic model most accurately describes the SO_2 adsorption onto the nanocomposite.

The principle of high adsorption capacity of $\text{MgO}/\text{AC}/\text{CaCO}_3/\text{Zeolite}$ nanocomposite relates to the nanomaterials that are combined in the adsorbent layer. The finding results indicated that compared to traditional adsorbents, which were often made of AC [27], compounds MgO , CaCO_3 , and zeolite are effective in increasing the efficiency of the adsorbent layer. In a similar study, Wang et al. [28] illustrated the mechanism for the heterogeneous oxidation of SO_2 to sulfate on the MgO surface. They showed that SO_2 was adsorbed with an active lattice oxygen atom or two oxygen atoms through the sulfur atom and formed the sulfite and sulfate on the perfect and step sites of the MgO surface, respectively. Conversion of sulfite to sulfate on the MgO surface is critically dependent on the presence of O_2 . Another study reported an efficient SO_2 adsorbent material prepared by calcination of natural magnesite [29]. The authors of the mentioned work described the SO_2 adsorption process on MgO as a chemisorption process, resulting in the surface formation of magnesium sulfite and magnesium sulfate over MgO -based adsorbents. Osaka et al. [30] showed that CaCO_3 was capable of effectively adsorbing SO_2 gas at low-temperature conditions. Fig. 14 illustrates the various chemical reactions that occur between SO_2 gas and the components of the $\text{MgO}/\text{AC}/\text{CaCO}_3/\text{Zeolite}$ nanocomposite adsorbent layer. The main reaction here is between MgO and SO_2 to yield MgSO_3 . Such a reaction in flue gas desulfurization processes involves the use of MgO as an effective sorbent for SO_2 capture. Moreover, the presence of CaCO_3 within the nanocomposite can further increase the general efficiency of SO_2 capture via further reactions, which might

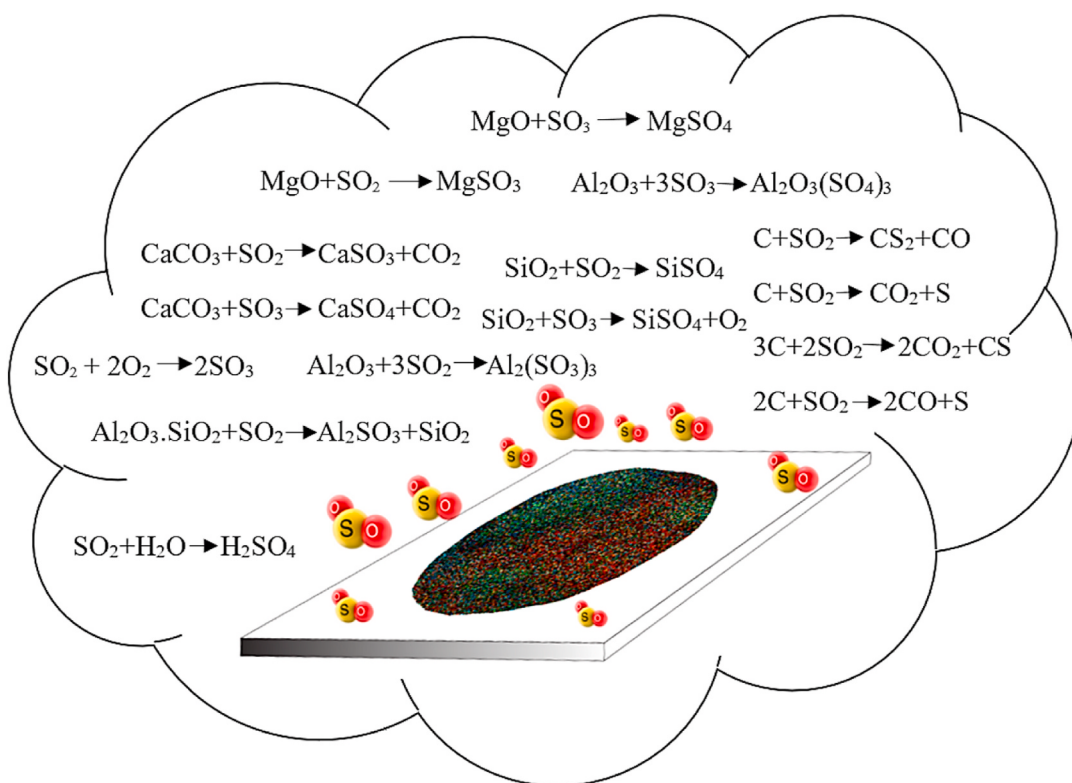


Fig. 14. The chemical reactions of SO_2 gas on the adsorbent film.

Table 1
Comparison of the SO_2 gas removal by various nanocomposites.

Materials	Gas	Temperature (°C)	Time (minute)	E (%)	Ref.
MgO/AC/CaCO ₃ /Zeolite	SO ₂	RT	5	92	This work
MnO ₂ /Mg-Al LDH	SO ₂	800	>10 ^a	42	[31]
MnO ₂ /Mg-Al LDH	SO ₂	170	>80 ^a	20	[32]
MgO/AC	SO ₂	RT	100 ^a	80	[33]
PVA/GO	SO ₂	RT	300 ^a	60	[34]
Activated coke/Potassium	SO ₂	RT	12 ^a	90	[35]
Activated coke	SO ₂	RT	5 ^a	90	[36]
Activated coke/V ₂ O ₅	SO ₂	200	>150 ^a	30	[37]

^a Extracted from the curves.

result in the formation of CaSO_3 or MgSO_4 when MgSO_3 becomes oxidized. The AC and zeolite components in the nanocomposite also contribute to the adsorption and retention of SO_2 , improving the overall performance of the adsorbent layer. Such a combination enables fast SO_2 removal.

Different studies on the removal of SO_2 gas are compared with the present research and reported in Table 1. To perform a better comparison, materials of the adsorbent layer, temperature condition, adsorption time, and efficiency are compared in Table 1. As shown in Table 1, the MgO/AC/CaCO₃/Zeolite nanocomposite exhibited the highest efficiency of 92 % after 5 minutes at room temperature. A study investigated the thermal decomposition characteristics of MnO₂/Mg-Al layered double hydroxide (LDH) [31]. The structure of LDH allows for the intercalation of anions, which balances the positive charge within the host layer. LDH exhibits significant anion exchange properties, making it suitable for applications in ion exchange systems and catalytic processes. That study achieved an efficiency of 42 % at 800 °C. In another study, a film composed of MnO₂/Mg-Al LDH demonstrated an

efficiency of 20 % when subjected to a temperature of 170 °C [32]. Comparison of MgO/AC/CaCO₃/Zeolite adsorbent layer with MnO₂/Mg-Al LDH studies exhibited the nanocomposite showed a fast absorption time in low operating temperatures and higher efficiency. Przepiorski et al. [33] studied the application of MgO-loaded porous carbon as a hybrid sorbent for SO_2 removal from air streams. Their results indeed testified to the presence of MgSO_3 and MgSO_4 on the surface of the MgO. They further asserted that the MgO/AC attained 80 % SO_2 removal efficiency at lower temperatures after 100 minutes. A comparison of the MgO/AC/CaCO₃/Zeolite adsorbent layer with the MgO/AC study exhibited the nanocomposite showed a faster absorption time and higher efficiency that can be related to the effectiveness of the CaCO₃/Zeolite. Ref. [34] reported the synthesis of PVA/GO nanocomposite membranes for SO_2 pollutants mitigation. A characteristic property of these nanocomposite membranes is that they hold a good potential to be active adsorbents in applications involved with removing SO_2 pollutants. It follows that optimized PVA/GO membranes had a 60 % removal after 5 h which showed a 60-fold slower absorption time compared to the nanocomposite.

Activated coke adsorption represents a feasible method for the simultaneous removal of gaseous pollutants such as SO_2 , NO_x , and volatile organic compounds. Qie et al. [35] proposed an eco-friendly potassium-assisted catalytic activation technique to prepare coal-based activated cokes for SO_2 gas removal. They showed that the adsorbent layer reached an efficiency of 90 % after 12 minutes. Another study presented that the microporous coke realized SO_2 adsorption capacity at 33 mg g^{-1} with 90 % in 5 minutes [36]. Research has also identified that AC materials have excellent abilities in the simultaneous capture of several pollutants. The V₂O₅/AC catalyst material prepared with activated coke-supported vanadia is also identified to have the SO_2 gas adsorption capacity of 90 % at a temperature of 200 °C [37]. Table 1 shows that the nanocomposite exhibited a better performance compared to various types of activated coke compounds.

4. Conclusion

Different industries are researching the potential of nanocomposites for reducing harmful gases, especially from industrial emissions and vehicles. It is important to develop materials that are capable of both detecting and absorbing various kinds of air pollutants to improve environmental protection. Various technologies, including adsorption, absorption, catalytic reduction, biological treatment, and injection of dry sorbent, are used to rid the atmosphere of pollutant gases. Each of these methods has inherent limitations that must be considered in choosing an appropriate air pollution control strategy. This research presents the application of an innovative nanocomposite featuring the MgO/AC/CaCO₃/Zeolite adsorbent layer for the efficient elimination of SO₂ gas. The nanocomposite exhibited a remarkable efficiency of 92 % within 5 minutes at room temperature. The nanocomposite demonstrated a significant adsorption capacity, quantified at 138 mg g⁻¹. The chemical reactions suggest the generation of sulfide, sulfate, and sulfuric acid on the adsorbent layer, which could cause a decrease in the adsorption capacity. Comparison of MgO/AC/CaCO₃/Zeolite adsorbent layer with other studies exhibited the nanocomposite showed a fast absorption time in low operating temperatures and higher efficiency. Research concentrating on the absorption of SO₂ within nanocomposite materials has yielded encouraging findings, indicating significant advantages in eliminating pollutants.

CRediT authorship contribution statement

Ghobad Behzadi pour: Writing – original draft, Supervision, Methodology. **Maryam Kamel Oroumiyah:** Investigation, Data curation. **Leila Fekri aval:** Validation, Methodology, Formal analysis.

Declaration of competing interest

The authors declare that they have no known competing financial interests or personal relationships that could have appeared to influence the work reported in this paper.

Acknowledgments

This research work was supported by the Department of Physics, East Tehran Branch, Islamic Azad University, Tehran, Iran, and the Science and Research Branch, Islamic Azad University, Tehran, Iran.

Data availability

Data will be made available on request.

References

- [1] I. Larki, A. Zahedi, M. Asadi, M.M. Forootan, M. Farajollahi, R. Ahmadi, A. Ahmadi, Mitigation approaches and techniques for combustion power plants flue gas emissions: a comprehensive review, *Sci. Total Environ.* 903 (2023) 166108, <https://doi.org/10.1016/j.scitotenv.2023.166108>.
- [2] R. Cui, S. Ma, B. Yang, S. Li, T. Pei, J. Li, J. Wang, S. Sun, C. Mi, Simultaneous removal of NOx and SO₂ with H₂O₂ over silica sulfuric acid catalyst synthesized from fly ash, *Waste Manag.* 109 (2020) 65–74, <https://doi.org/10.1016/j.wasman.2020.04.049>.
- [3] L. Luo, Y. Guo, T. Zhu, Y. Zheng, Adsorption species distribution and multicomponent adsorption mechanism of SO₂, NO, and CO₂ on commercial adsorbents, *Energy Fuels* 31 (10) (2017) 11026–11033, <https://doi.org/10.1021/acs.energyfuels.7b01422>.
- [4] X. He, Y. Chen, J. Gao, F. Wang, B. Shen, Research progress and application prospects of modified clay materials for flue gas pollutants purification, *Appl. Clay Sci.* 258 (2024) 107483, <https://doi.org/10.1016/j.clay.2024.107483>.
- [5] E.F. Mohamed, F. Mohamed, A. El-Mekawy, W. El Hotaby, Development of PVA/GO nanocomposites membranes for air-filtration and purification, *J. Inorg. Organomet. Polym. Mater.* 33 (11) (2023) 3389–3401, <https://doi.org/10.1007/s10904-023-02762-1>.
- [6] G. Behzadi pour, S. Motamed, A.H. Sari, L. Fekri aval, Plasma effect on the NO, CO, and SO₂ gases pollutant removal using AC/MgO/Fe₂O₃/TiO₂/ZnO/zeolite nanocomposite, *Case Studies Chem. Environ. Eng.* 10 (2024) 100890, <https://doi.org/10.1016/j.cscee.2024.100890>.
- [7] Sh. Khatami, L. Fekri Aval, G. Behzadi Pour, Investigation of nanostructure and optical properties of flexible AZO thin films at different powers of RF magnetron sputtering, *Nano* 13 (6) (2018) 1850062, <https://doi.org/10.1142/s1793292018500625>.
- [8] G. Behzadi, H. Golnabi, Monitoring temperature variation of reactance capacitance of water using a cylindrical cell probe, *J. Appl. Sci.* 9 (4) (2009) 752–758, <https://doi.org/10.3923/jas.2009.752.758>.
- [9] G. Behzadi, L. Fekri, Electrical parameter and permittivity measurement of water samples using the capacitive sensor, *Int. J. Water Resour. Environ. Sci.* 2 (3) (2013) 66–75, <https://doi.org/10.5829/idosi.ijwres.2013.2.3.2938>.
- [10] S. Khatami, G.B. Pour, S.F. Aval, M. Amini, Cold atmospheric plasma brush effect on population reduction of different bacterial spectrums, *Plasma Chem. Plasma Process.* 43 (5) (2023) 1131–1147, <https://doi.org/10.1007/s11090-023-10354-7>.
- [11] Y.F. Avval, G.B. Pour, M.M. Aram, Fabrication of high efficiency coronavirus filter using activated carbon nanoparticles, *Int. Nano Lett.* 12 (4) (2022) 421–426, <https://doi.org/10.1007/s40089-022-00379-9>.
- [12] G. Behzadi pour, L. Fekri aval, Recent advances in supercapacitors based on MXene surface modification: a review of symmetric and asymmetric electrodes material, *Result Eng.* 24 (2024) 103045, <https://doi.org/10.1016/j.rineng.2024.103045>.
- [13] G.B. Pour, H.N. Fard, L.F. Aval, D. Dubal, Recent advances in Ni-Materials/Carbon nanocomposites for supercapacitor electrodes, *Mater. Adv.* 4 (23) (2023) 6152–6174, <https://doi.org/10.1039/d3ma00609c>.
- [14] W. Wen, C. Wen, D. Wang, G. Zhu, J. Yu, P. Ling, M. Xu, T. Liu, A review on activated coke for removing flue gas pollutants (SO₂, NO_x, Hg₀, and VOCs): preparation, activation, modification, and engineering applications, *J. Environ. Chem. Eng.* 12 (2) (2024) 111964, <https://doi.org/10.1016/j.jece.2024.111964>.
- [15] C. Wen, W. Wen, D. Wang, Z. Jing, Q. Liu, M. Xu, G. Zhu, Research progress on removal of flue gas pollutants by activated coke, *Clean Coal Tech.* 29 (1) (2023) 83–107, <https://doi.org/10.13226/j.issn.1006-6772.T22111201>.
- [16] J. Zhou, H. Wang, Study on efficient removal of SO_x and NO_x from marine exhaust gas by wet scrubbing method using urea peroxide solution, *Chem. Eng. J.* 390 (2020) 124567, <https://doi.org/10.1016/j.cej.2020.124567>.
- [17] M. Yu, S. Zeng, Y. Nie, X. Zhang, S. Zhang, Ionic liquid-based adsorbents in indoor pollutants removal, *Curr. Opin. Green Sustainable Chem.* 27 (2021) 100405, <https://doi.org/10.1016/j.cogsc.2020.100405>.
- [18] Q.-Y. Li, D.-Q. Hu, J. Zhang, X. Gao, Synergistic removal of WFGD and WESP on gas pollutants with ultra low emission, *J. Eng. Therm. Energy Power* 32 (8) (2017) 138–143, <https://doi.org/10.16146/j.cnki.rndlgc.2017.08.022>.
- [19] D. Xia, C. He, L. Zhu, Y. Huang, H. Dong, M. Su, M.A. Asi, D. Bian, A novel wet-scrubbing process using Fe(vi) for simultaneous removal of SO₂ and NO, *J. Environ. Monit.* 13 (4) (2011) 864, <https://doi.org/10.1039/c0em00647e>.
- [20] M. Zheng, L. Shen, J. Xiao, Reduction of CaSO₄ oxygen carrier with coal in chemical-looping combustion: effects of temperature and gasification intermediate, *Int. J. Greenh. Gas Control* 4 (5) (2010) 716–728, <https://doi.org/10.1016/j.ijggc.2010.04.016>.
- [21] B. He, X. Zheng, Y. Wen, H. Tong, M. Chen, C. Chen, Temperature impact on SO₂ removal efficiency by ammonia gas scrubbing, *Energy Convers. Manag.* 44 (13) (2003) 2175–2188, [https://doi.org/10.1016/s0968-8904\(02\)00230-3](https://doi.org/10.1016/s0968-8904(02)00230-3).
- [22] G. Behzadi pour, E. Shahjehnia, E. Darabi, L. Fekri aval, H. Nazarpour-Fard, E. Kianfar, Fast NO₂ gas pollutant removal using CNTs/TiO₂/Cu/O/zeolite nanocomposites at the room temperature, *Case Studies Chem. Environ. Eng.* 8 (2023) 100527, <https://doi.org/10.1016/j.cscee.2023.100527>.
- [23] B. Tanhaei, A. Ayati, M. Lahtinen, M. Sillanpää, Preparation and characterization of a novel chitosan/Al₂O₃/magnetite nanoparticles composite adsorbent for kinetic, thermodynamic and isotherm studies of methyl orange adsorption, *Chem. Eng. J.* 259 (2015) 1–10, <https://doi.org/10.1016/j.cej.2014.07.109>.
- [24] B. Sizirci, I. Yıldız, Adsorption capacity of iron oxide-coated gravel for landfill leachate: simultaneous study, *Int. J. Environ. Sci. Technol.* 14 (5) (2016) 1027–1036, <https://doi.org/10.1007/s13762-016-1207-9>.
- [25] N. Mozaffari, A. Hajji Seyed Mirzahosseini, A.H. Sari, L. Fekri Aval, Investigation of carbon monoxide gas adsorption on the Al₂O₃/Pd(NO₃)₂/zeolite composite film, *J. Theoret. Appl. Phys.* 14 (1) (2019) 65–74, <https://doi.org/10.1007/s40094-019-00360-6>.
- [26] S.A. Idris, K.M. Alotaibi, T.A. Peshkur, P. Anderson, M. Morris, L.T. Gibson, Adsorption kinetic study: effect of adsorbent pore size distribution on the rate of Cr (VI) uptake, *Microporous Mesoporous Mater.* 165 (2013) 99–105, <https://doi.org/10.1016/j.micromeso.2012.08.001>.
- [27] N. Karatepe, İ. Orbak, R. Yavuz, A. Özyügüran, Sulfur dioxide adsorption by activated carbons having different textural and chemical properties, *Fuel* 87 (2008) 3207–3215, <https://doi.org/10.1016/j.fuel.2008.06.002>.
- [28] H. Wang, C. Zhong, Q. Ma, J. Ma, H. He, The adsorption and oxidation of SO₂ on MgO surface: experimental and DFT calculation studies, *Environ. Sci.: Nano* 7 (2020) 1092–1101, <https://doi.org/10.1039/c9en01474h>.
- [29] Q. Zhang, Q. Tao, H. He, H. Liu, S. Komarneni, An efficient SO₂-adsorbent from calcination of natural magnesite, *Ceram. Int.* 43 (2017) 12557–12562, <https://doi.org/10.1016/j.ceramint.2017.06.130>.
- [30] Y. Osaka, F. Takahashi, T. Tsujiguchi, A. Kodama, H.Y. Huang, Z.H. He, H.H. Taoli, Development of SO₂ absorption materials having low temperature activity by base adducted complex method, *Adv. Mater.* 960–961 (2014) 65–68, <https://doi.org/10.4028/www.scientific.net/amr.960-961.65>.
- [31] T. Kameda, T. Kurutach, Y. Takahashi, S. Kumagai, Y. Saito, S. Fujita, I. Itou, T. Han, T. Yoshioka, Thermal decomposition behavior of MnO₂/Mg-Al layered double hydroxide after removal and recovery of acid gas, *Resul. Chem.* 4 (2022) 100310, <https://doi.org/10.1016/j.rechem.2022.100310>.

- [32] T. Kameda, Y. Takahashi, S. Kumagai, Y. Saito, S. Fujita, I. Itou, T. Han, T. Yoshioka, Study of dynamics and mechanism of HCl, SO₂, or NO removal by MnO₂/Mg-Al layered double hydroxide, Inorg. Chem. Commun. 135 (2022) 109108, <https://doi.org/10.1016/j.inoche.2021.109108>.
- [33] J. Przepiórski, A. Czyżewski, J. Kapica, D. Moszyński, B. Grzmil, B. Tryba, S. Mozia, A.W. Morawski, Low temperature removal of SO₂ traces from air by MgO-loaded porous carbons, Chem. Eng. J. 191 (2012) 147–153, <https://doi.org/10.1016/j.cej.2012.02.087>.
- [34] E.F. Mohamed, F. Mohamed, A. El-Mekawy, W. El Hotaby, Development of PVA/GO nanocomposites membranes for air-filtration and purification, J. Inorg. Organomet. Polym. Mater. 33 (11) (2023) 3389–3401, <https://doi.org/10.1007/s10904-023-02762-1>.
- [35] Z. Qie, F. Sun, Z. Zhang, X. Pi, Z. Qu, J. Gao, G. Zhao, A facile trace potassium assisted catalytic activation strategy regulating pore topology of activated coke for combined removal of toluene/SO₂/NO, Chem. Eng. J. 389 (2020) 124262, <https://doi.org/10.1016/j.cej.2020.124262>.
- [36] Z. Qie, Z. Zhang, F. Sun, L. Wang, X. Pi, J. Gao, G. Zhao, Effect of pore hierarchy and pore size on the combined adsorption of SO₂ and toluene in activated coke, Fuel 257 (2019) 116090, <https://doi.org/10.1016/j.fuel.2019.116090>.
- [37] Q. Liu, Z. Liu, Carbon supported vanadia for multi-pollutants removal from flue gas, Fuel 108 (2013) 149–158, <https://doi.org/10.1016/j.fuel.2011.05.015>.